2013 IEEE Signal Processing in Medicine and Biology Symposium (SPMB), Polytechnic Institute of New York University, New York, NY, 7 December, 2013.

EMG-Force Estimation for Multiple Fingers

Pu Liu, Donald R. Brown and *Edward A. Clancy
Department of Electrical and Computer Engineering
Worcester Polytechnic Institute, Worcester, MA, U.S.A
{puliu, drb, ted}@wpi.edu

Francois Martel and Denis Rancourt
Department of Mechanical Engineering
University of Sherbrooke, Sherbrooke, Quebec, Canada
{Francois.Martel2, Denis.Rancourt}@USherbrooke.ca

***Abstract*—Electromyogram (EMG) activity from the extensor and flexor muscles of the forearm was sensed with high-density surface electrode arrays and related to the force produced at the four fingertips during constant-posture, slowly force-varying contractions from three healthy subjects. Various electrode montages (spatial filters) and number of electrodes used in the system identification were studied. Average errors were small, ranging from 4.21 to 8.10 %MVC$_F$ (flexion maximum voluntary contraction), with errors trending lower when more EMG channels were used and when a monopolar electrode montage was selected. Results are supportive that multiple degrees of freedom of proportional control information are available from the surface EMG of the forearm, at least in intact subjects. Applications for future study include the control of prosthetic upper limb devices in amputees.**

Keywords—Biological system modeling; electromyography; EMG signal processing; biomedical signal processing.

I. INTRODUCTION

Numerous research studies have attempted to relate the electromyogram (EMG) activity of the forearm muscles to the mechanical activity of the wrist, hand and/or fingers. A primary interest is for EMG control of powered upper-limb prostheses, with additional interests including ergonomic analysis of manual tasks and clinical neuromuscular evaluation. The long-term goal for prosthetic control is to provide a replacement limb with functionality and control similar to that of an intact limb, i.e. "… simultaneous, independent, and proportional control of multiple degrees of freedom …" [1]. Existing commercial EMG-controlled powered hand prostheses are limited to rudimentary control capabilities of either three discrete states (open, close, off) or one degree of freedom of proportional control [1]. To extend control capabilities, several classification schemes using inputs from conventional surface EMG electrodes have been demonstrated in various laboratory conditions for discriminating between 5–10 hand/wrist functions [2]–[8] or for classification of individual finger movements [9]–[13]. Classification accuracy above 95% has been reported in some conditions, with accuracy decreasing as the number of classes increases, the number of EMG electrodes decreases and the window length of the EMG processor decreases. These methods may provide for increased amputee function, even though continuous proportional control of movement is generally not achieved. Some studies of finger movement have considered proportional control via EMG-based estimation of finger forces or finger joint angles [13]–[15].

Supported by U.S. Army under USAMRAA Grant W81XWH-08-1-0422.

Many studies have approached this problem while limiting the number of EMG electrodes and the amount of computer computation, since prosthesis-based solutions must fit into low power, low weight, portable systems. However, advances in EMG electrode technology and low power microprocessors are rapidly making these concerns moot, and such concerns are not as pressing in ergonomic and medical applications. In recent years, high resolution spatial filtering of surface EMG has been used to localize electrical potentials to small volumes of muscle tissue [16]–[18]. These systems are attractive for the small muscles of the forearm, in order to reduce EMG cross-talk that might hinder signal separation from functionally distinct muscles that lie in close proximity.

In this report, we describe a laboratory study that relates forearm flexor and extensor EMG to flexion-extension force generated at the tips of the four fingers (index, middle, ring, pinky) during constant-posture, slowly force-varying contractions. A high resolution EMG array was applied over the flexion and extension muscles of the forearm, and various spatial filters were utilized to enhance signal separation. The project goal was to assess the ability to determine two or more degrees of freedom of control from the agonist-antagonist muscles of the forearm.

II. METHODS

A. Experimental Apparatus

The experimental apparatus consisted of a restraint device for constant-posture finger flexion-extension, a custom LabView interface for acquisition and real-time display of finger forces, and a commercial EMG amplifier array and acquisition system. The finger restraint and an EMG electrode array are shown in Fig. 1. The experimental apparatus and procedures were approved by the New England Institutional Review Board, an IRB of record for Worcester Polytechnic Institute.

The finger restraint was custom built using modular framing (10 Series Profiles, 80/20 Inc., Columbia City, IN, U.S.A.). As shown in Fig. 1, the restraint contained a rectangular base with outer dimensions of 20 by 45 cm, with extensions that were rigidly clamped to a heavy table. The subject sat along the table edge with their elbow forming a 90^o angle. A cushioned elbow rest plate was mounted at the rear of the base. The location of this plate (distance from the restraint upright) was adjusted for each subject such that the forearm was only supported by the olecranon process. The EMG electrodes, once mounted on the forearm, were never in contact

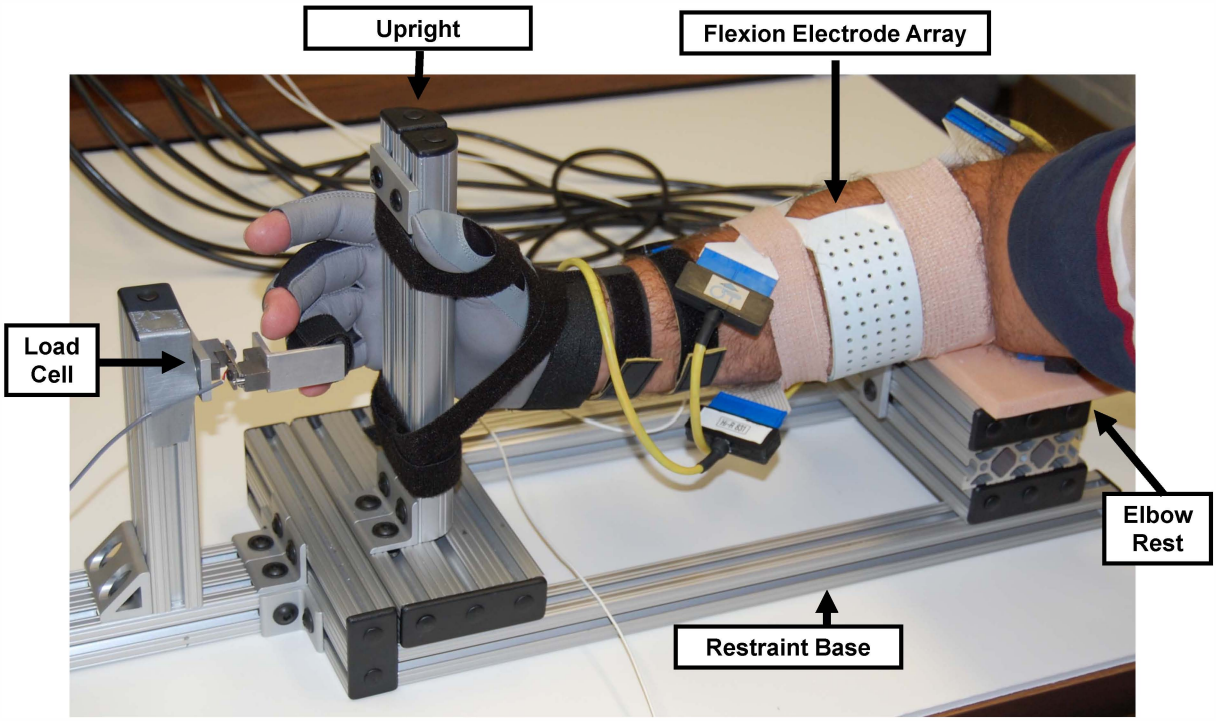

Fig. 1. Photograph of hand/arm secured into the finger restraint. A Velcro strap is wrapped around one finger (the fourth digit is used in this photo) to secure it to the load cell, which measures finger flexion-extension. The gloved hand is held to the restraint upright using Velcro. Electrode arrays are mounted over the medial (flexion array) and lateral (extension array—not visible) aspects of the forearm.

with the finger restraint. The height of the elbow rest plate was also adjusted for each finger to keep the long axis of the forearm parallel to the table. After donning a glove, the palm of the hand was secured to the front of the restraint to an upright, using Velcro. The glove adhered to the Velcro better than the bare hand and prevented the need to actively stabilize the hand during contractions of a finger. The hand was oriented with the thumb directed upwards and the four remaining digits passively curled and extending beyond the upright. The height of the hand above the base could be adjusted so that the distal phalange of any one of the four remaining digits was aligned with the load beam. A phalange was secured to the load beam by wrapping a thin Velcro strip around the beam and distal phalange. The load on this beam was measured with a one degree of freedom load cell and amplifier (Load Cell Model LCL-040, Amplifier Model DMD-465WB; Omega Engineering, Inc., Stamford, CT, U.S.A.). The cut-off frequency of the amplifier lowpass filter was set at 9.4 Hz (second-order, Bessel). A constant-posture flexion force was directed towards the restraint upright and an extension force was directed away. Measurement was only made on one digit at a time. The load cell amplifier was re-zeroed before each contraction to prevent drift during the experiment. Between trials, subjects were released from the Velcro restraints, as needed, so as to maintain normal circulation to the hand.

For EMG recordings, the skin over the circumference of the proximal right forearm was scrubbed with an alcohol wipe. Two, 64-channel monopolar electrode arrays and their associated commercial amplification-acquisition system recorded the EMG (ELSCH064R3S Adhesive Electrode Arrays, EMG-USB Amplifier; OT Bioeletronica, Torino, Italy). Each array was a rectangular, 13x5 matrix of electrodes (with one corner electrode omitted), utilizing 2 mm diameter electrodes (gel-filled) separated by 8 mm (center-to-center). The long axis of the "flexion" array was oriented and secured along the circumference of the right forearm, centered on the mid-line of the medial aspect of the forearm. The omitted corner electrode was closest to the base of the finger restraint, in the most proximal electrode column. The second "extension" array was secured with the long axis oriented along the right forearm circumference, centered on the mid-line of the lateral aspect of the forearm. The omitted corner electrode was closest to the base of the finger restraint, in the most distal electrode column. The eight extension electrodes located furthest from the base of the finger restraint along the most proximal electrode column were not recorded, leaving 56 electrodes. A gap of 3.5–7 cm existed between the two electrode arrays, both at the restraint base and 180° along the forearm circumference. The proximal edge of each EMG array was located three fingers width from the olecranon process [19]. A wrist-band reference electrode was applied to the left wrist. Two wrist-band electrodes were also used to operate a "driven-right-leg" interference attenuation circuit. Both of these electrodes were applied to the right arm, typically distal to the recording electrodes. Each electrode channel had a gain of 20,000, a bandwidth extending from 10–750 Hz, a CMRR greater than 104 dB at the power line frequency, an input impedance greater than 10^{14} Ω, and an input referred noise of less than 1 μV RMS. EMG data were sampled within the commercial amplifier system at 2048 Hz using a 12-bit ADC, and then transferred to a dedicated PC that controlled operation of the EMG system. As a measure of total EMG system noise, data from the three electrode rows closest to the muscle mid-line were analyzed while subjects relaxed their arm completely.

The recorded signal's MAV level, containing equipment noise as well as ambient physiological activity, averaged 9.44 ± 5.48% of the MAV EMG at 30% maximum voluntary contraction (MVC).

A second PC was used to collect the finger flexion-extension load cell data (after amplification) and as a subject display. The 18 inch monitor of this PC was placed approximately 1 m in front of the subject. A custom LabView interface displayed a vertical line on the screen that moved horizontally with the subject's extension-flexion force. A fixed or dynamic target could also be displayed on the screen as well as a text box indicating the voltage level corresponding to the instantaneous force exerted by the subject. The flexion-extension load cell data were acquired at 128 Hz using a 16-bit ADC (model PCI6229, National Instruments, Austin, TX, U.S.A.). In addition, a signal generator was used to produce a 1 V, 0.5 Hz sine wave. This sine wave was simultaneously acquired by the LabView PC and EMG array hardware, and utilized off-line to time synchronize the data recordings from these two devices.

B. Experimental Methods

Three subjects successfully completed one experiment each. Subjects had no known neuromuscular deficits of their right hand, arm or shoulder. Each subject was instructed to relax all muscles not directly involved in the task, and to maintain consistent postures and contraction techniques for each finger throughout all trials. After signing written informed consent, subjects were fitted into the hand restraint device. Subjects warmed up and accommodated to the contraction task by producing force against the load cell separately with each digit, followed by a three minute rest period to avoid fatigue. Thereafter, each subject performed separate maximum flexion, then extension trials for each of the four digits, repeated twice. For each contraction, subjects began at rest and then took 2–4 s to ramp force up to their maximum. The plateau maximum that was maintained for approximately 1 s was recorded. Consistent verbal encouragement was provided for each trial. The average flexion plateau for each digit and the average extension plateau for each digit were used as the respective MVC values. Subsequent contractions were scaled to the MVC of the respective digit.

The EMG electrode arrays were then secured to the forearm, as detailed above. Subjects then performed a series of slowly force-varying tracking tasks. The LabView display of extension-flexion force was scaled over the range from 30% MVC extension to 30% MVC flexion. A target signal on the screen began at the force level half-way between these two extremes (this level was not equivalent to zero force, since extension and flexion MVCs are not equal in magnitude), advanced to 30% extension, continued to 30% flexion, returned to 30% extension, and ended back at the half-way force. This tracking lasted 30 s, with all target movement at a constant speed equal to 6% MVC_{Ave} per second, where MVC_{Ave} is the average of the flexion and extension MVCs. Four tracking tasks were completed per digit. A typical experiment lasted approximately three hours. Explicit rest was not provided between exertion trials, since adequate rest to prevent localized fatigue was provided by only utilizing one digit per trial and rotating through the digits.

C. Methods of Analysis

Data Preprocessing: All data analysis was performed off-line using MATLAB (The MathWorks, Natick, MA). The sampled EMG data were bandpass filtered (15–700 Hz) using a fourth-order Butterworth filter, and second-order notch filters at the power line frequency and all harmonics (due to the presence of significant power line interference). Filtering was applied in the forward, then reverse time directions to achieve zero phase. Each data recording was plotted and reviewed. Channels with anomalous data (e.g., obviously corrupted by excessive power line noise or motion artifact) were marked and avoided from further use. Nonetheless, all desired electrode configurations were achieved. The finger force data were upsampled to the same rate as the EMG data (2048 Hz), time-aligned to the EMG data and scaled to its respective flexion MVC value (MVC_F). The fingertip force for inactive fingers was set to zero.

EMG-Force Using Classic Spatial Filters: The EMG-force model is shown in Fig. 2. Numerous classic spatial filters with known (pre-selected) spatial filter coefficients were investigated. The preprocessed extensor/flexor signal sets ($e_{E,i}[n]$, $e_{F,i}[n]$, where i indexes the spatial channels and n indexes time) were spatially filtered to produce L extensor/flexor channels ($m_{E,i}[n]$, $m_{F,i}[n]$). A spatial filter is a memory-less weighted sum of the monopolar potentials. The EMG standard deviation (EMG amplitude estimate) of each channel was computed by rectifying each channel and then decimating to 10.24 Hz. After decimating, the signal was further lowpass filtered (cut-off frequency of 1 Hz, fourth-order Butterworth filter applied in the forward, then reverse time directions), producing signals $EMG\sigma_{E,i}[m]$ and $EMG\sigma_{F,i}[m]$, where m indexes time at the reduced rate. The first and last five seconds of each 30 s tracking trial were discarded, to eliminate filter startup transients, leaving one complete contraction cycle of duration 20 s per digit. Four sequential tracking recordings, representing data from each of the four digits, were concatenated to form an 80 s data set. A fit coefficient was multiplied by each of the L extension EMGσ's to estimate each of the four digit extension force contributions (total of $4L$ coefficients). Another $4L$ coefficients were similarly required to estimate flexion force contributions. Their difference was the estimate of total force for each finger. Linear least squares was used to estimate the fit coefficients from an 80 s tracking set. Four tracking data sets were available per subject. Three data sets were used for coefficient training and the fourth for performance testing, with full leave-one-out cross-validation. The average error from the four cross-validations was expressed in percent MVC flexion (%MVC_F), relative to each respective digit.

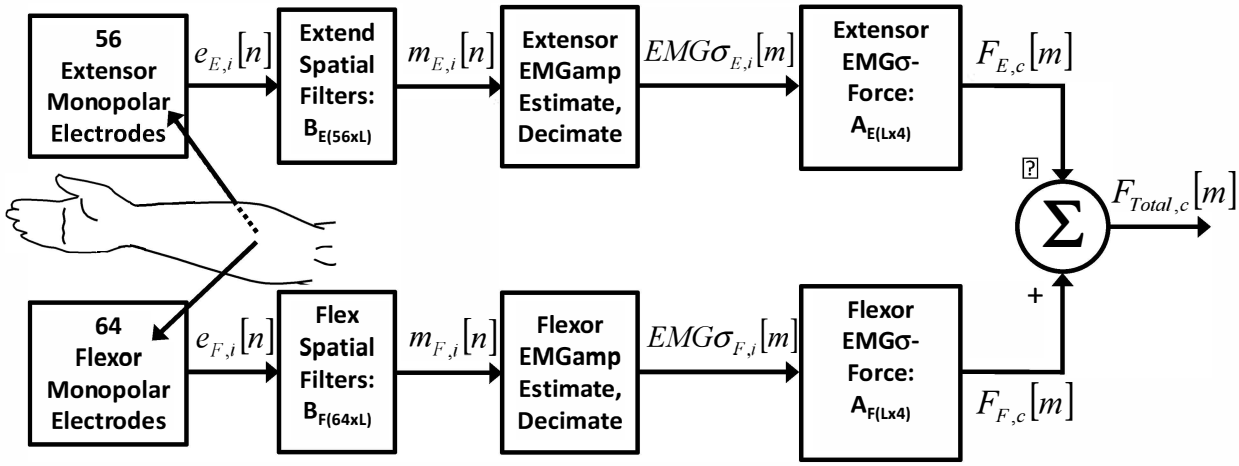

Fig. 2. EMG-force model. Each of the 56 extension and 64 flexion monopolar arrays are spatially filtered into *L* signals, each signal being used to produce one EMG standard deviation (EMGσ) estimate at the reduced sampling rate. Least squares estimation is then used to simultaneously relate the EMGσ's to force of the four (or selections of two) fingertips (indexed by *c*). Sample index *n* denotes signals at the rate of 2048 Hz, while sample index *m* denotes signals at the rate of 20.48 Hz. The "*B*" matrices hold the coefficients of the spatial filters, while the "*A*" matrices hold the coefficients relating EMGσ to torque.

Each extension/flexion EMG array contained 13 rows of electrodes. An *L*=13 channel monopolar spatial filter (montage) was formed by choosing one of the central electrodes in each row. Then, alternate rows were selected to form an *L*=7 channel monopolar spatial filter. By skipping increasingly more rows, filters were formed for *L*=5 and 4 channels. Next, these four row selections were repeated, utilizing additional adjacent columns to form bipolar and linear double difference (LDD) filters [16]. Note that these filters were formed along the presumed direction of action potential propagation. Lastly, normal double difference (NDD) filters were formed. Because of the additional rows required to form NDD filters, the selected channel sizes were *L*=11, 6 and 4. Thus a total of 15 classic spatial filters were investigated.

Models were initially formed relating the EMG channels simultaneously to forces in all four fingers. Modeling was then repeated to relate the EMG channels to force in each pair of fingers, of which there were six combinations (index-middle, index-ring, index-pinky, middle-ring, middle-pinky, ring-pinky).

III. Results

Fig. 3 shows sample results using a monopolar montage of 13 electrode channels per extension and flexion array. The pinky finger seems to exhibit the most independent control and the index finger the least. Table I shows RMS error results for the various electrode montages and number of channels, when force was simultaneously estimated in *all four* fingertips. The trend was for lower error when more EMG channels were used and when the monopolar montage was selected. In many applications, as few as two degrees of freedom of proportional control would represent a significant control advantage. Thus, Table II shows RMS error results for each *pair* of fingers for various electrode montages, using the maximum number of channels. The trend was for lower errors when using the monopolar montage and when one of the fingers in a pair was the pinky finger. All of these errors are similar in general magnitude to EMG-force errors found in studies of other joints (c.f., [20]). Given the small number of subjects (three), statistical comparisons were not pursued.

IV. Discussion

Although the sample size was small, the results showed relatively small EMG-force errors, averaging 4.21–8.10 $\%MVC_F$, depending on the number of electrode channels and the montage used. The evidence from this research work, as well as prior research (see the Introduction section) suggests that surface EMG activity from the forearm encodes multiple degrees of freedom of proportional control information that may be sufficient for use in controlling prosthetic wrists, hands and/or fingers—*at least when tested on intact subjects*. It would, therefore, seem appropriate to encourage investigation of the use of these EMG-force algorithms in amputees. It seems important to determine if the extent of information and control available in the intact forearm is also available in the remnant forearm muscles of amputees. In an off-line, four-class study, Hudgins *et al.* [5] found an average ± standard deviation classification accuracy of 91.2% ± 5.6% for able-bodied subjects and 85.5 ± 9.8% for amputees. In an off-line, 11-class study of amputees, Li *et al.* [6] found a classification accuracy of 94% ± 3% with the intact arm vs. 79% ± 11% with the amputated arm. Real-time evaluation using a virtual prosthesis showed additional performance deficits comparing the amputated side to the intact side. The reason(s) for the lower performance in these studies from the amputated side is unclear. Perhaps damage to the remnant muscle tissue has adversely altered the anatomy through reduced muscle mass, altered muscle locations, scar tissue (which insulates the EMG signal from the surface electrodes), or other affects. Alternatively, perhaps the loss of afferent receptors in the amputated arm hinders calibration of the EMG-based controllers (e.g., it is difficult for subjects to repeat a task with precision when joint torques cannot be measured)—an issue that might be alleviated through repetitive training.

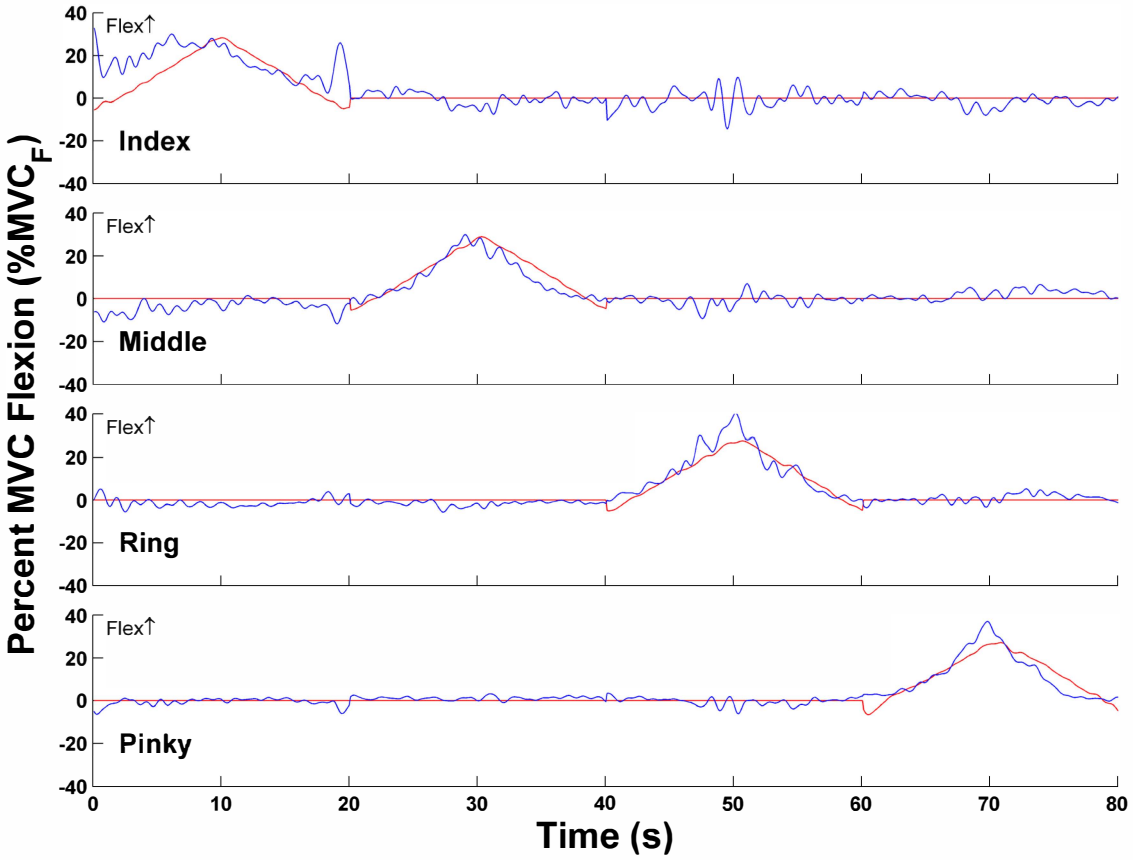

Fig. 3. Sample EMG-force test results of estimated (jagged blue line) and actual (solid red line) force vs. time using L=13 monopolar montage. Four, 20 s ramp trials are combined to form each plot. Each finger is only active for one 20-s portion and resting otherwise. Subject WY04, trials 22, 23, 32, 33.

TABLE I
AVERAGE RMS TEST ERROR RESULTS (%MVC$_F$) FROM THREE SUBJECTS FOR FINGERTIP TRACKING TRIALS WHEN ESTIMATING FORCES IN **FOUR** FINGERS SIMULTANEOUSLY

EMG Channels (L)	Spatial Filter			
	Mono	Bipolar	LDD	NDD
13 (11 for NDD)	4.41	5.49	5.97	5.51
7 (6 for NDD)	4.51	5.68	5.73	5.58
5	4.69	5.37	5.91	—
4	4.84	5.45	5.99	5.51

TABLE II
AVERAGE RMS TEST ERROR RESULTS (%MVC$_F$) FROM THREE SUBJECTS FOR FINGERTIP TRACKING TRIALS WHEN ESTIMATING FORCES IN **TWO** FINGERS SIMULTANEOUSLY, 13 EMG CHANNELS (11 FOR NDD)

Finger Pair	Spatial Filter			
	Mono	Bipolar	LDD	NDD
Index-Middle	5.82	8.10	7.72	7.60
Index-Ring	5.59	6.30	**6.14**	**5.51**
Index-Pinky	5.41	6.34	7.01	5.91
Middle-Ring	5.03	5.93	6.16	6.80
Middle-Pinky	**4.21**	5.85	6.79	6.46
Ring-Pinky	4.81	**5.81**	7.28	7.71

This study was intended as an initial assessment of EMG-force estimation in the fingers. As such, several study limitations should be noted. First, data were only analyzed from three subjects. Additional subjects would improve generalizability of the results. Second, subjects only produced constant-posture, slowly force-varying contractions. It is well known that the EMG-force relationship varies with posture [21], [22] and with force dynamics [23], [24]. Third, the performance of EMG-force models has seen little testing relative to the influences of localized muscle fatigue, electrode movement and day-to-day variations (when applicable). Fourth, the electrode arrays used in this project are not appropriate for use in reusable systems (such as prosthetics) that are routinely donned and doffed by their user. The system was selected for its large number of active electrodes, with the understanding that knowledge learned in this study might direct research towards a more deployable electrode solution in the future. Fifth, the spatial filters derived in software from the acquired monopolar EMG channels do not have characteristics identical to hardware-based spatial filters. In particular, software-derived EMG signals tend to contain higher common-mode interference (thus, our need to notch filter the power-line and its harmonics—losing a portion of the usable EMG spectrum in the process) and the smaller surface area of the array electrodes tend to exhibit more random (background) measurement noise [25]. Nonetheless, we selected a high resolution surface array to take advantage of its small inter-electrode distance (to improve selectivity), which is generally not available with conventional bipolar surface EMG systems (due to the risk of electrode shorting, among other concerns). Future EMG-based prosthesis control systems might achieve high selectivity and better noise/interference performance via indwelling electrodes [26], [27]. Lastly, our modeled relationship between forearm EMG and finger forces does not include thumb movement, thus leaving ambiguity as to how

several common hand motions (e.g., key grip, pinch grip), or even concomitant wrist activation, might be controlled. In this study, we have concentrated on determining available degrees of freedom of independent, proportional control, expecting that future research would determine how those signals might be fully utilized to control a prosthesis (or be utilized in other applications).

V. Conclusion

EMG signals were acquired from the extensor and flexor muscles of the forearm during constant-posture, slowly force-varying contractions and related to the force produced in the four fingers (index, middle, ring and pinky). Various conventional electrode montages and number of EMG channels were considered. Over a range of contraction forces spanning 30% MVC extension to 30% MVC flexion, RMS EMG-force error ranged from 4.21–8.10 $\%MVC_F$, depending on the montage and number of channels. Errors tended to be lower when more channels were used and when the monopolar montage was selected. Results were encouraging for forearm EMG-force applications in areas such as prosthesis control and ergonomic analysis.

References

[1] P. A. Parker, K. Englehart and B. Hudgins, "Myoelectric signal processing for control of powered limb prostheses," *J. Electromyo. Kinesiol.*, vol. 16, pp.541–548, 2006.

[2] K. Englehart, B. Hudgins and P. A. Parker, "A Wavelet-Based Continuous Classification Scheme for Multifunction Myoelectric Control," *IEEE Trans. Biomed. Eng.*, vol. 48, pp.302–311, 2001.

[3] K. A. Farry, I. D. Walker and R. G. Baraniuk, "Myoelectric Teleoperation of a Complex Robotic Hand," *IEEE Trans. Robot. Automat.*, vol. 12, pp. 775–788, 1996.

[4] B. Karlik, M. O. Tokhi and M. Alci, "A Fuzzy Clustering Neural Network Architecture for Multifunction Upper-Limb Prosthesis," *IEEE Trans. Biomed. Eng.*, vol. 50, pp.1255–1261, 2003.

[5] B. Hudgins, P. A. Parker, R. N. Scott, "A New Strategy for Multifunction Myoelectric Control," *IEEE Trans. Biomed. Eng.*, vol. 40, pp.82–94, 1993.

[6] G. Li, A. E. Schultz and T A. Kuiken, "Quantifying Patter Recognition-Based Myoelectric Control of Multifuntional Transradial Prostheses," *IEEE Trans. Biomed. Eng.*, vol. 18, pp. 185–192, 2010.

[7] P. Shenoy, K. J. Miller, B. Crawford and R. P. Rao, "Online Electromyographic Control of a Robotic Prosthesis," *IEEE Trans. Biomed. Eng.*, vol. 55, pp. 1128–1135, 2008.

[8] M. Zecca, S. Micera, M. C. Carrozza and P. Dario, "Control of Multifunctional Prosthetic Hands by Processing the Electromyographic Signal," *Crit. Rev. Biomed. Eng.*, vol. 30, pp. 459–485, 2002.

[9] A. Andrews, E. Morin and L. McLean, "Optimal Electrode Configurations for Finger Movement Classification using EMG," *Proc. 31st Ann. Int. Conf. IEEE EMBS*, 2009, pp. 2987–2990.

[10] J. Z. Wang, R. C. Wang, F. Li, W. Jiang and D. W. Jin, "EMG Signal Classification for Myoelectric Teloperating a Dexterous Robot Hand," *Proc. 27th Ann. Int. Conf. IEEE EMBS*, 2005, pp. 5931–5933.

[11] D. Peleg, E. Braiman, E. Yom-Tov and G. F. Inbar, "Classification of Finger Activation for Use in a Robotic Prosthesis Arm," *IEEE Trans. Neural Sys. Rehab. Eng.*, vol. 10. pp. 290–293, 2002.

[12] F. V. G. Tenore, A. Ramos, A. Fahmy, S. Acharya, R. Etienne-Cummings and N.V. Thakor, "Decoding of Individuated Finger Movements Using Surface Electromyography," *IEEE Trans. Biomed. Eng.*, vol. 56, pp. 1427–1434, 2009.

[13] C. Castellini and P. van der Smagt, "Surface EMG in Advanced Hand Prosthetics," *Bio. Cyber.*, vol. 100, pp. 35–47, 2009.

[14] R. J. Smith, D. Huberdeau, F. Tenore and N. V. Thakor, "Real-Time Myoelectric Decoding of Individual Finger Movements For a Virtual Target Task," *Proc. 31st Ann. Int. Conf. IEEE EMBS*, 2009, pp. 2376–2379.

[15] R. J. Smith, F. Tenore, D. Huberdeau, R. Etienne-Cummings and N. V. Thakor, "Continuous Decoding of Finger Position from Surface EMG Signals for the Control of Powered Prostheses," *Proc 30th Ann. Int. Conf. IEEE EMBS*, 2008, pp. 197–200.

[16] C. Disselhorst-Klug, J. Bahm, V. Ramaekers, A. Trachterna and G. Rau, "Non-invasive approach of motor unit recording during muscle contractions in humans," *Eur. J. Appl. Physiol.*, vol. 83, pp. 144–150, 2000.

[17] H. Reucher, G. Rau and J. Silny, "Spatial Filtering of Noninvasive Multielectrode EMG. I: Introduction to Measuring Technique and Implications," *IEEE Trans. Biomed. Eng.*, vol. 34, pp. 98–105, 1987.

[18] H. Reucher, J. Silny and G. Rau, "Spatial Filtering of Noninvasive Multielectrode EMG. II: Filter performance in theory and modeling," *IEEE Trans. Biomed. Eng.*, vol. 34, pp. 106–113, 1987.

[19] A. O. Perotto, *Anatomical Guide for the Electromyographer.* Third edition, Springfield, IL: Charles C Thomas, 1994, pp. 30–73.

[20] E. A. Clancy, L. Liu, P. Liu and D. V. Z. Moyer, "Identification of Constant-Posture EMG-Torque Relationship About the Elbow Using Nonlinear Dynamic Models," *IEEE Trans. Biomed. Eng.*, vol. 59, pp. 205–212, 2012.

[21] Z. Hasan and R. M. Enoka, "Isometric torque-angle relationship and movement-related activity of human elbow flexors: Implications for the equilibrium-point hypothesis," *Exp. Brain Res.*, vol. 59, pp. 441–450, 1985.

[22] J. Vredenbregt and G. Rau, "Surface electromyography in relation to force, muscle length and endurance," *New Developments in Electromyogr., Clin. Neurophysiol.*, vol. 1, pp. 607–622, 1973.

[23] G. L. Gottlieb and G. C. Agarwal, "Dynamic relationship between isometric muscle tension and the electromyogram in man," J. App. Physiol., vol. 30, pp 345–351, 1971.

[24] E. A. Clancy, O. Bida and Denis Rancourt, "Influence of advanced electromyogram (EMG) amplitude processors on EMG-to-torque estimation during constant-posture, force-varying contractions," *J. Biomech.*, vol. 39, pp. 2690-2698, 2006.

[25] R. Merletti and H. Hermens, "Detection and Conditioning of the Surface EMG Signal," in *Electromyography: Physiology, Engineering, and Noninvasive Applications.* Hoboken, NJ: R. Merletti and P. A. Parker (eds.), John Wiley & Sons, Inc., 2004, pp. 107–131.

[26] J. J. Baker, E. Scheme, K. Englehart, D. T. Hitchinson and B. Greger, "Continuous Detection and Decoding of Dexterous Finger Flexions with Implantable MyoElectric Sensors," *IEEE Trans. Rehab. Eng. Neural Sys.*, vol. 18, pp. 424–432, 2010.

[27] M. Lowery, R. F. Weir and T. A. Kuiken, "Simulation of Intramuscular EMG Signals Detected Using Implantable Myoelectric Sensors (IMES)," *IEEE Trans. Biomed. Eng.*, vol. 53, pp. 1926–1933, 2006.